International Journal of Mechanical Sciences 244 (2023) 108087

Contents lists available at ScienceDirect

International Journal of Mechanical Sciences

journal homepage: www.elsevier.com/locate/ijmecsci

Unveiling the damage evolution of SAC305 during fatigue by entropy generation

Xu Long [a,*], Ying Guo [a], Yutai Su [a,*], Kim S. Siow [b], Chuantong Chen [c]

[a] School of Mechanics, Civil Engineering and Architecture, Northwestern Polytechnical University, Xi'an, China
[b] Institute of Microengineering and Nanoelectronics, Universiti Kebangsaan Malaysia, Selangor, Malaysia
[c] Institute of Scientific and Industrial Research, Osaka University, Osaka, Japan

ARTICLE INFO

Keywords:
Mechanical fatigue
Entropy generation
Peak stress
Damage parameter
Microstructure

ABSTRACT

Low-cycle thermal-mechanical fatigue loadings induce progressive and permanent degradation of mechanical properties of lead-free solder materials, and thus reduce the fatigue life of electronic devices. In this study, damage evolution and accumulation of Sn-3.0Ag-0.5Cu (SAC305), the most successfully commercialized lead-free solder material, was investigated by performing strain-controlled fatigue tests at different temperatures (288–373 K) and strain rates (0.001–0.004 s^{-1}). Unlike existing empirical models, a fatigue damage model was proposed based on entropy generation related to the thermodynamic nature of fatigue damage. To be intrinsic to entropy generation, the proposed model was calibrated with the peak stress degradation at different temperatures and strain rates. Our findings showed that the damage parameter is closely related to temperature and strain rate and monotonically increases from 0 to 1 during the low-cycle fatigue loading, which unveiled the fact regarding the irreversibility of the internal entropy generation. For the first time, the damage evolution is found to be more associated with the applied strain rate than the temperature. By observations using an optical microscopy, the physical damage mechanism is elucidated for SAC305 solder by correlating microstructures and damage evolutions. The evolving dendritic β-Sn phase and the surrounding Sn-Ag-Cu ternary eutectic network also explained the effects of temperature and strain rate based on the energy dissipation. Our proposed damage model reconciled the damage accumulation of SAC305 solder subjected to the low-cycle fatigue loading, which is readily adopted to predict the fatigue life of the electronic packaging structures.

1. Introduction

Solder materials play an increasingly crucial role in the electronics interconnection structures with the rapid development of electronic packaging technology. The mechanical reliability of these packaging structures also determines the service lifetime of the entire device or system, especially under harsh application conditions [1–3]. Therefore, selecting and describing the mechanical properties of solder materials has become crucial from a practical and reliability viewpoint.

The Pb-free solders are widely used in the consumer electronics industry instead of the Pb-containing solders because of their harmful effects on the environment and human health. Sn-3.0Ag-0.5Cu (SAC305) Pb-free solder has been recommended as an alternative to Pb-Sn solder in the National Electronics Manufacturing Initiative since 2000 because of its low melting temperature and good mechanical reliability [4,5]. Hence, accurately and quickly assessing the fatigue damage of the Pb-free solder materials is becoming a crucial issue in achieving packaging structures with a high-performance and high-mechanical reliability for critical applications. In crucial applications, repeated power on/off and high-frequency vibration cause cyclic loadings and stresses on electrical devices. This thermal cycling and the mismatch of the coefficients of thermal expansion of different layered materials leads to thermal fatigue failures of packaging structures; this failure concentrates at the solder joints, which undergo accumulative damage and permanent degradation [6–8].

Fatigue is essentially a process consisting of the formation, aggregation, and growth of micro-cracks during the cyclic loading, leading to strength reduction and, ultimately fracture failure. There have been many research activities in the existing literature to predict the fatigue evolution of Pb-free solders under different loading conditions [5,9–16]. It is generally accepted that the numerical prediction of fatigue life for solder materials typically consists of four major steps, as reviewed by

* Corresponding authors.
E-mail addresses: xulong@nwpu.edu.cn (X. Long), suyutai@nwpu.edu.cn (Y. Su).

https://doi.org/10.1016/j.ijmecsci.2022.108087
Received 31 May 2022; Received in revised form 27 December 2022; Accepted 27 December 2022
Available online 29 December 2022

Lee et al. [17]. Firstly, a constitutive model is selected to describe the mechanical behaviour of solder materials in the finite element simulations of packaging structures. Secondly, the mechanical responses (*i.e.*, stress, strain, plastic strain, etc.) of the solder materials are calculated by applying the cyclic loading, which is identical to that under experimental conditions. Thirdly, the obtained mechanical responses are examined to identify the critical solder joints. Finally, the fatigue life can be estimated using the selected fatigue life prediction model, which is validated based on the experimental data.

It can be found that fatigue damage and life assessment methods for solder structures mainly contain Miner's cumulative damage law [18], damage mechanics method [19–21] and probability method [22,23]. Among them, the damage mechanics method is more advantageous to describe the damage of the material or structure, but has limitations to determine the complex relationship between the degree of damage and the stress state [24]. The probabilistic method can provide a comprehensive analysis for a good number of uncertainties affecting fatigue, but its drawback is the requirement of a large amount of test data as the basis for analysis [25]. The Miner's cumulative damage method is the most widely used, which can effectively assess the proportion of damage caused by different temperatures and strain rates, but its assessment results may apparently different from the actual cases if no detailed investigations are performed [26]. Therefore, great effects have been made to develop various improved or derived Miner's cumulative damage models, such as the bilinear damage model and the nonlinear damage model [27–32]. In general, low-cycle fatigue life predictions for Pb-free solder in the existing literature were usually based on stress and strain, which essentially belong to curve fitting models or phenomenological models, such as the Coffin-Manson model and Morrow model [12,13,33–36]. For instance, the Coffin-Manson model was adopted based on experimental data to correlate the amplitude of cyclic plastic deformation with the cycle numbers, which has been proven suitable for low-cycle fatigue problems for solder joint materials [36–39]. Additionally, Liang et al. [9] provided a comprehensive review of multiaxial fatigue life prediction models to predict the multiaxial ratcheting–fatigue life. Nevertheless, it should be noted that these prediction models are empirical and thus cannot unveil the physical nature of the fatigue process of viscoplastic solder materials, especially the underlying mechanism of damage evolution and accumulation.

If any component and structure are considered as a thermodynamic system, the energy conversion efficiency is definitely less than 100% because of the inevitable energy dissipation based on Newtonian mechanics and the second law of thermodynamics. With the target to directly reflect the nature of damage accumulation until fatigue fracture, the thermodynamic entropy can be adopted to describe the degree of system disorderliness during the material fatigue process and also predict the fatigue life from a microscopic perspective. Thus, recent works developed a new fatigue damage model based on the entropy-generation theory. Hwang et al. [40] proposed an energy-based damage model for simulating low cycle fatigue for structural stainless steels by modifying existing models. They validated the proposed damage model by comparing it with through-wall cracked pipe tests of stainless steel. Because of plastic deformation during fatigue, energy dissipation can be quantified by entropy generation, which increases until its final ultimate value during cyclic loading. This phenomenon regarding the increasing entropy generation during fatigue loading is observed for various types of materials [41–43]. Recently, Samal and Moharana [44] analysed the physical properties of the recharging microchannel from the perspective of entropy generation. Their results showed that the entropy generation, as a thermodynamic quantity, can be reasonably assumed to be related to the fatigue evolution of the material specimen. In addition, uniaxial fatigue experiments of carbon steel by Jang and Khonsari [45] showed that the fracture fatigue entropy (FEE), as an intrinsic material property, indicates an accumulative entropy up to the fracture point. Similarly, Amiri and Khonsari [41], Naderi et al. [46], and Liakat and Khonsari [47] confirmed that the FEE of metal material failure remains constant at low- and high-cycle fatigue, while the FEE value is independent on external factors such as specimen geometry and loading amplitude. Thus, the entropy-based damage model is promising to unveil the underlying mechanism and make predictions with more physical significance for fatigue failure. It can be seen from the above critical review about the existing damage models [12,13,33–39], curve-fitting models based on experimental data are essentially empirical. Therefore, they cannot explain the physical nature of the fatigue process, especially the underlying damage evolution and accumulation. Fundamentally different from the empirical damage models, the entropy-based damage model is superior from a physical point of energy dissipation and is more potential to reveal fatigue damage along with the observation of microscopic evolution [48–50], and put forward a new fatigue damage model based on entropy-generation theory. Therefore, the present study makes the first attempt to propose an entropy-based damage model for predicting the damage accumulation of the viscoplastic solder materials.

In recent years, the concept of entropy has been adopted for the complex systems working under mechanical fatigue, thermal loading, and wear conditions based on mechanical thermodynamics [51–53]. Some entropy-based fatigue models were proposed to characterize the fatigue life of composite materials [54–57]. However, there are only a few studies in the existing literature on the entropy-based fatigue models for Pb-free solders. In the present study, low-cycle fatigue experiments were performed on SAC305 specimens at a maximum strain of 0.12, subjected to different temperatures and strain rates. The entropy generation was derived as a damage parameter based on the Newtonian mechanics and the second law of thermodynamics. Then, the variables in the damage model were correlated to temperatures and strain rates, in combination with the strength degradation under different cyclic loading conditions. Finally, the damage evolution was reconciled to confirm the accuracy of the proposed entropy-generation damage model with the accumulative damage data generated during the mechanical-cyclic loading. This result has never been realized for Pb-free solder materials to the best of our knowledge. To further elucidate the microscopic evolution of SAC305 under different cyclic conditions, the microstructure of SAC305 after fatigue tests was also characterized by an optical microscope. Therefore, the damage model is proposed to provide a basis for coupling with the unified creep plasticity model [58–60] through UMAT subroutine in the future. On the basis of this, the damage accumulation during mechanical cycling of viscoplastic solder can be simulated by finite element simulation software to obtain the equivalent plastic strain increment PEEQ, and finally the fatigue life of the material can be evaluated by Coffin-Manson model.

2. Experimental and theoretical methods

This section presents the experimental and theoretical methods for exploring the fatigue damage of SAC305 under low-cycle fatigue. The material specification, specimen preparation and fatigue loading method are described. The framework of the proposed damage model is derived based on the entropy-generation.

2.1. Materials preparation and experimental procedure

The chemical composition of the purchased SAC305 Pb-free solder rods from Alpha Assembly Solutions (New Jersey, US) is shown in Table 1, and the solder rods were cut into rectangular specimens with the dimensions of 69.8, 3.0 and 5.0 mm, respectively, by the low-speed wire-cut electrical discharge machining. Then, the specimens were further prepared by chamfering for the transition regions and the surfaces were smoothened by using the high-speed milling cutter. Eventually, the dog-bone shaped SAC305 specimens were obtained as shown in Fig. 1, which has a surface finish of 0.8 μm Ra to satisfy the practical requirement for those parts that are exposed to stress concentration. According to the existing natural aging methods [61–64] to release the residual stress and stabilize the microstructures, the solder specimens

Table 1
Chemical composition of SAC305 solder (wt.%).

Solder type	Sn	Ag	Cu	Pb	Sb	As	Fe	Ni	Al	Zn
SAC305	Bal.	3.0	0.5	<0.08	<0.05	<0.03	<0.02	<0.01	<0.002	<0.002

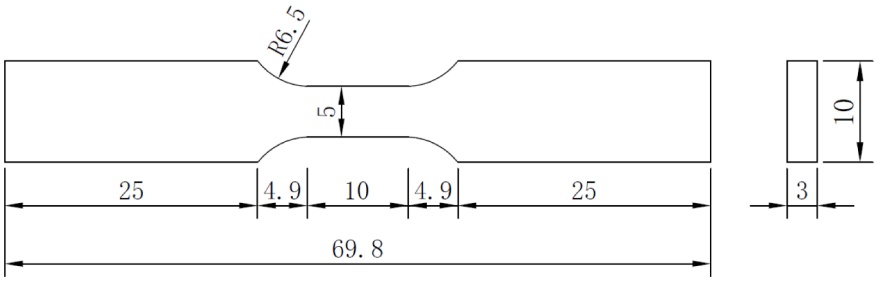

Fig. 1. Geometry of dog-bone shaped specimen of SAC305 Pb-free solder to investigate the monotonic tensile behaviour and damage evolution during the fatigue tests (unit: mm).

were stored at the room temperature and in a dry environment for more than 20 days to relieve the residual stress caused by the machining process [65].

Then, the solder samples were tested in a universal testing machine by SUNS Inc. (Shenzhen, China) with a temperature chamber under strain-controlled cyclic conditions for up to 400 cycles at constant temperatures and strain rates. Different testing temperatures were selected, *i.e.*, 288 K, 308 K, 343 K and 373 K, and the corresponding strain rates were chosen, *i.e.*, 0.001 s^{-1}, 0.002 s^{-1} and 0.004 s^{-1}, respectively, to cover all typical loading scenarios of mechanical reliability assessment.

Based on the soldering and packaging processes, residual strains remained in the solder joints of electronic packaging structures to influence the fatigue life of solder joints under the service conditions. According to the monotonic tensile behaviour in Fig. 2, it can be found that SAC305 solder has clearly entered the plastic stage when the strain reaches 0.12 by uniaxial tensile experiments at different temperatures. This means that the damage definitely exists and accumulates at the tensile strain of 0.12, which can also be a representative working condition when the solder material undergoes excessive stress due to installation or CTE mismatch of electronic packaging structures. Therefore, this study prescribed a tensile strain of 0.12 for the SAC305 solder specimens before applying the strain amplitude of 0.01 during the strain-controlled fatigue tests. Subsequently, all fatigue experiments at different temperatures were performed using a triangular waveform loading path with different strain rates, as shown in Fig. 3. In light of the fact that fatigue behaviour exhibits significant scatter, the average values and standard deviations of three duplicate specimens for each testing condition are shown in Fig. 4. The apparent peak stress differences of experimental results confirm the damage differences due to different temperatures and strain rates. The average value was considered the reliable experimental data for the damage analysis and the calibration of the proposed entropy fatigue model. Furthermore, it should be noted that applied low-cycle fatigue deformation at a quasi-static state was consistent with the actual applications of solder materials in electronic packaging structures [65].

For the solder microstructure characterization, the solder specimens, after being tested for 400 cycles, were sectioned in the middle of the gauge length using a precision cutting machine at a low speed of 400 rpm. Then, metallographic grinding and polishing machines were used with the diamond pastes (0.3 μm and 0.05 μm) to polish the samples to reach a mirror-like surface for the solder sample. To reveal different phases of the microstructures on the solder, the polished solder specimens were etched with a mixed solution of 2% HCl + 3% HNO_3 + 95% C_2H_2OH (vol.%) for 9 s [66]. Finally, the specimens were cleaned in an ultrasound bath of ethanol for 3 min to remove any diamond paste and chemical residue left from the polishing and etching process. Optical

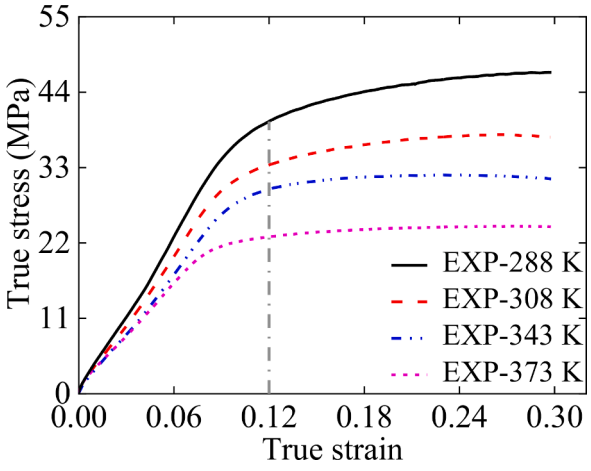

Fig. 2. Monotonic tensile behaviours of the specimens of SAC305 solder by uniaxial tensile experiments at four different temperatures of 288 K, 308 K, 343 K, and 373 K respectively.

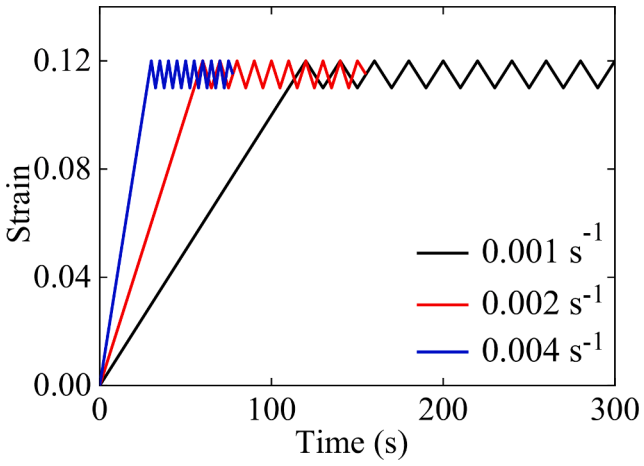

Fig. 3. Strain-controlled cyclic loading paths for different strain rates of 0.001 s^{-1}, 0.002 s^{-1}, and 0.004 s^{-1} in uniaxial fatigue tests of SAC305 solder specimens, which were conducted with the same prescribed tensile strain of 0.12 and strain amplitude of 0.01 to identify the effects of temperatures and strain rates.

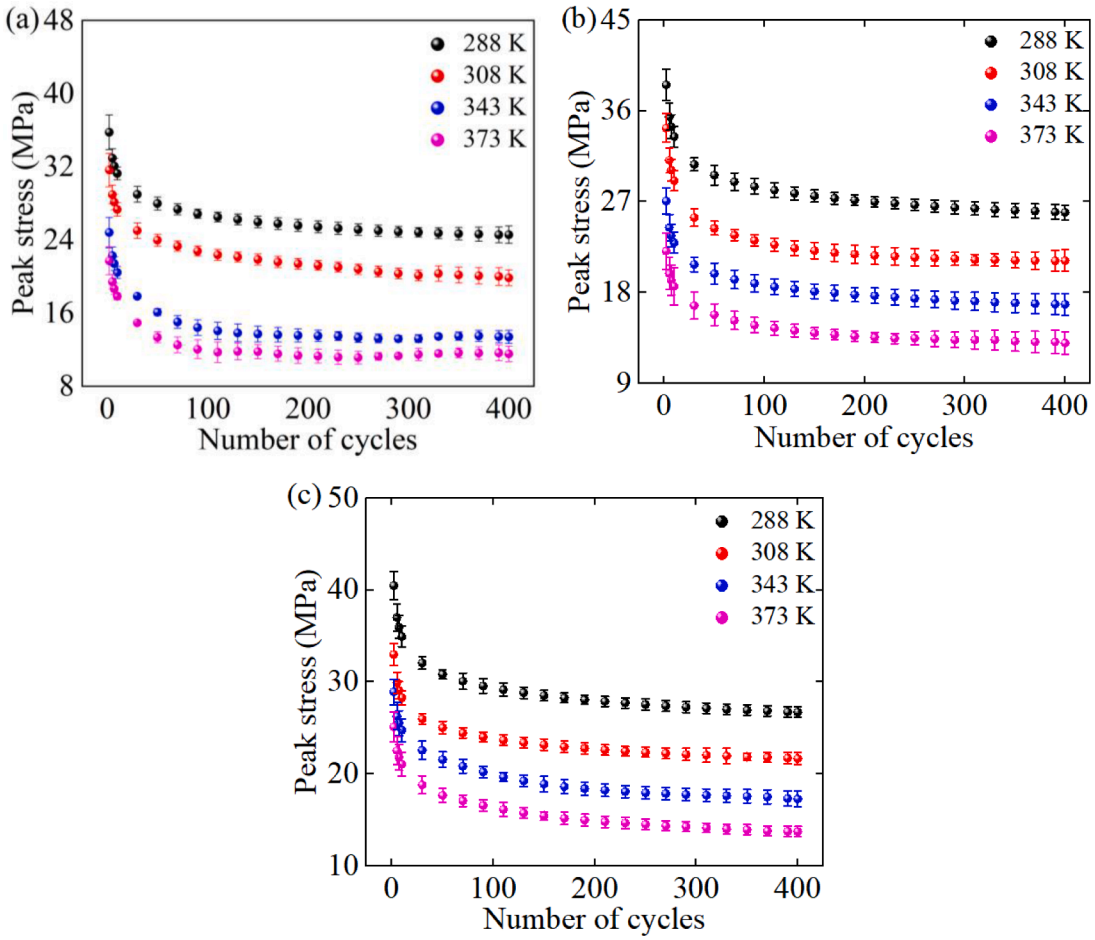

Fig. 4. Average values and standard deviations of experimental data obtained at temperatures of 288 K, 308 K, 343 K, and 373 K for strain rates of (a) 0.001 s^{-1}, (b) 0.002 s^{-1}, and (c) 0.004 s^{-1}, respectively. The insets illustrate the authenticity and reliability of the data from this experiment.

microscopy (Model ISH500 from Tucsen, Fuzhou, China) was used to capture micrographs at representative locations of the solder specimens.

2.2. Framework of the proposed entropy-generation damage model

It is reasonable to assume that the energy dissipation is quantified by the strength reduction caused by cyclic loading. In addition, entropy generation is a quantity larger than zero, indicating the accumulation of energy dissipation during the irreversible process of the thermodynamic system. In terms of governing equation, Temfack and Basaran [67] presented the range and trend of damage parameters based on the thermodynamic laws, and verified them with uniaxial cyclic and monotonic loading. Based on the internal energy and entropy change perspectives, the internal entropy generation γ is based on the change of the total entropy in the system of a solder specimen, and can be expressed as

$$\gamma = \frac{\boldsymbol{\sigma} : \boldsymbol{\varepsilon}^p}{T} + \frac{k}{T^2}\left|\overrightarrow{gradT}\right|^2 + \frac{\rho r}{T} \geq 0 \tag{1}$$

where $\boldsymbol{\sigma}$ represents the stress tensor, $\boldsymbol{\varepsilon}^p$ is the plastic strain, T is the temperature, ρ is the material density, r represents the specific internal heat source per unit time, and k is constant. In Eq. (1), the first term represents the plastic work done which incorporates the effect of mechanical loading, the second term represents the contribution by the thermal loading, and the last term represents the other types of loading acting on the solder specimen.

It is widely accepted that the damage parameter should be zero in the initial state before the fatigue deformation. The damage parameter gradually grows during the fatigue loading as the loading time increases. When the damage parameter reaches a critical value usually taken as the unit 1.0, the material specimen is considered to have failed due to the applied fatigue loading. Therefore, the internal entropy is first normalized to accommodate the damage evolution by characterizing the material property degradation during the mechanically cyclic loading. As the ratio of the change in the disorder parameter W to the initial state disorder parameter W_0, the damage parameter D is defined as [43, 68–70]

$$D = \frac{W_0 - W}{W_0} \tag{2}$$

In addition, a relationship between the disorder parameter W and the internal entropy s_i of the specimen system can be established as [42]

$$s_i = \frac{R}{\zeta \cdot m_s}\ln(\beta \cdot W), \tag{3}$$

where R is the gas constant, m_s represents the molar mass, ζ is the loading-related parameter to indicate the thermo-mechanical coupled effect, and β is a scaling factor to guarantee to be physically and mathematically compatible. After rewriting Eq. (3), Eq. (4) can be obtained as

$$W = \frac{1}{\beta}\exp\left(\zeta \cdot s_i \cdot \frac{m_s}{R}\right). \tag{4}$$

After substituting Eq. (4) into Eq. (2), the damage parameter can be further expressed as

$$D = \frac{W_0 - W}{W_0} = 1 - \exp\left[-\zeta \cdot (s_i - s_{i0}) \cdot \frac{m_s}{R}\right]. \quad (5)$$

Based on Eq. (4), when the internal entropy s_i is equal to the initial internal entropy s_{i0}, the damage parameter of the specimen system is 0 if the solder specimen does not have any existing initial damage. On the other hand, when the internal entropy s_i is infinity, the damage parameter equals 1, *i.e.*, the system solder specimen fails. This assumption is compatible with the commonly known fact that the thermodynamic system is regarded to fail before the damage parameter reaches 1 in most situations. According to Eq. (1), the term $s_i - s_{i0}$ can then be written in a generalized form as

$$s_i - s_{i0} = \Delta s_i = \int_{t_0}^{t} \frac{\gamma}{\rho} dt = \int_{t_0}^{t} \frac{\boldsymbol{\sigma} : \boldsymbol{\varepsilon}^p}{\rho T} + \frac{k}{\rho T^2} \left|\overrightarrow{grad} T\right|^2 + \frac{r}{T} dt. \quad (6)$$

Since the mechanical effect on the fatigue behaviour of SAC305 solder material is the main focus of the present study, the specimen temperature was maintained constant during the loading process. The specimen was only subjected to mechanically cyclic loading in a uniaxial direction. As a result, the second and third terms in Eq. (6) are no longer considered further for our analysis. As the damage parameter D is directly reflected by the reduction of peak stress in each loading cycle during the fatigue experiments, Eq. (6) can be rewritten as

$$s_i - s_{i0} = \Delta s_i = \int_{t_0}^{t} \frac{\boldsymbol{\sigma} : \boldsymbol{\varepsilon}^p}{\rho T} dt = \sum_{i=0}^{n} \frac{\Delta\sigma \cdot \Delta\varepsilon}{\rho T}, \quad (7)$$

where $\Delta\sigma$ represents the reduction of peak stress per loading cycle, $\Delta\varepsilon$ represents the strain amplitude for each cycle which is set as 0.02 in this study, and n is the number of cycles that is up to 400 as a low-cycle fatigue history.

To capture the degradation of measured peak stress during the fatigue loading, the continuum damage mechanics and the linear damage degradation are adopted from Krajcinovic [71]. Thus, the peak stress degradation can be described as

$$\sigma_{peak} = \sigma_{peak,0} \cdot (1 - D), \quad (8)$$

where $\sigma_{peak,0}$ and σ_{peak} are the peak stresses prior to and during fatigue deformation, respectively. Based on Eq. (8), the proposed damage parameter in Eq. (5) can be achieved from the peak stress degradation, providing the relationship between fatigue cycle number and solder material strength obtained from the performed experiments. These derivations suggest that the degradation of solder material strength is the consequence of entropy generation during the fatigue history.

3. Experimental results and damage model calibration

The proposed entropy-generation damage model describes the fatigue behaviour of SAC305 Pb-free solder materials. Therefore, the involved parameters of the damage model are calibrated against the experimental measurements from cyclically loaded material specimens at different temperatures and strain rates to confirm their applicable conditions. In addition, the evolution of the damage parameter D is elucidated under various loading conditions to verify the accuracy of the proposed entropy-generation damage model in capturing the fundamental accumulative damage during mechanical cyclic loading. This result is of interest to probe the underlying mechanisms of the damage-constitutive behaviour and provide the theoretical basis to numerical estimations for the fatigue life for Pb-free solder joints.

3.1. Effect of temperature and strain rate on damage

Experimental results are summarized from cyclically loaded material specimens at different temperatures and strain rates. The fatigue tests were performed in a strain-controlled manner, which facilitated the stress response in the time history to be obtained directly. The stress-strain relationship is derived further by associating the applied strain history in Fig. 5. Here, the stress at the maximum strain of 1.2 gradually decreases with increasing cycle numbers. Additionally, the envelope area in the center of the hysteresis loop becomes smaller as the cycle number increases, indicating the capacity deterioration of energy dissipation and thus confirming the accumulated damage during the fatigue test.

To derive the strength deterioration, the peak stress at each strain cycle is extracted to form the peak stress–cycle number responses to indicate the damage accumulation and entropy generation during the cyclic loading history. Fig. 6 shows the relationship between the cycle number and the peak stress for the entire loading history at various temperatures and strain rates with the same cyclic strain amplitude of 0.01. By inducing a significant reduction and subsequent stabilization of the peak stress for SAC305, the applied 400 strain cycles are sufficient to produce the damage evolution and accumulation.

Based on comparisons between the peak stresses at different temperatures and strain rates in Fig. 6, SAC305 solder demonstrates noticeable temperature softening and strain-rate hardening phenomenon. The deterioration trend of peak stress is similar to the previously reported experimental results by Long et al. [72]. The nonlinear relationship between peak stress and the cyclic number obtained from this experimental work proves that strength decreases significantly within the first 50 cycles. Then, the decrease gradually stabilizes because of the damage accumulation and entropy generation with the evolution of the damage parameter under different working conditions.

Furthermore, the difference between the initial peak stress and the stabilized peak stress increases with increasing temperature and strain rates, implying that the higher temperature or higher strain rate causes more significant for the same cycle number. Therefore, the temperature effect on damage is attributed to the increased energy dissipation for the same amount of time or the same number of cycles at higher temperatures. This result is consistent with the experimental results of other independent researches [73,74]. Similarly, the effect of strain rate on damage is attributed to the faster strain rates resulting in faster energy dissipation of SAC305 Pb-free solder for the same amount of time or number of cycles.

To quantify the fatigue damage at different temperatures, the relationship between the number of cycles and the peak stress can be further correlated by Eq. (8), as shown in Fig. 6, from which the results of damage parameters are obtained in Fig. 7 as the function of cycle number. It is noteworthy that it was observed that the most critical location was located in the middle of the gauge length by the

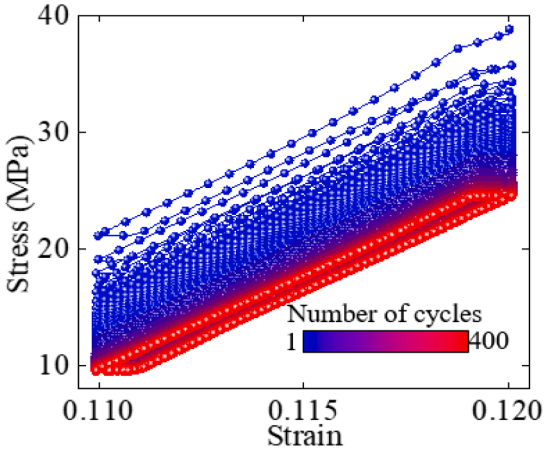

Fig. 5. Representative stress-strain relationship for the SAC305 solder specimen subjected to strain-controlled cyclic loading for a maximum of 400 cycles at a temperature of 288 K and a strain rate of 0.001 s^{-1}.

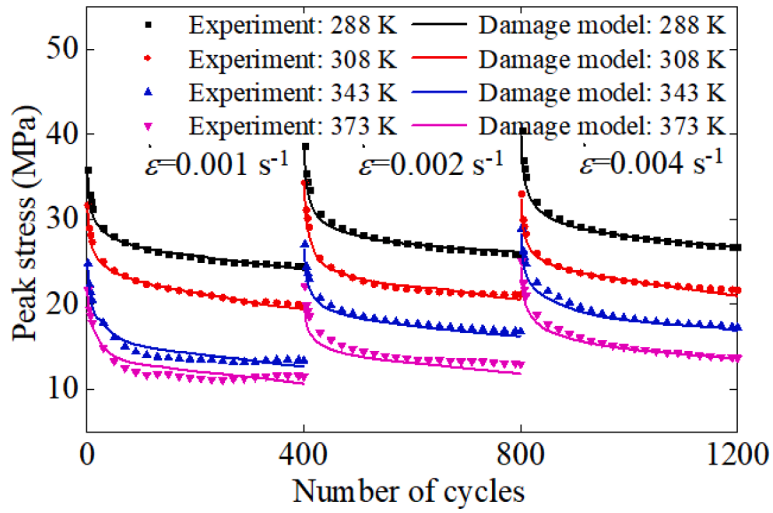

Fig. 6. Measured and predicted relationships between the number of cycles and peak stress at temperatures of 288 K, 308 K, 343 K, and 373 K, with the applied strain rates of 0.001 s^{-1}, 0.002 s^{-1}, and 0.004 s^{-1}. Noticeable effects of temperature softening and strain-rate hardening on SAC305 solder are demonstrated and simulated by the proposed damage model.

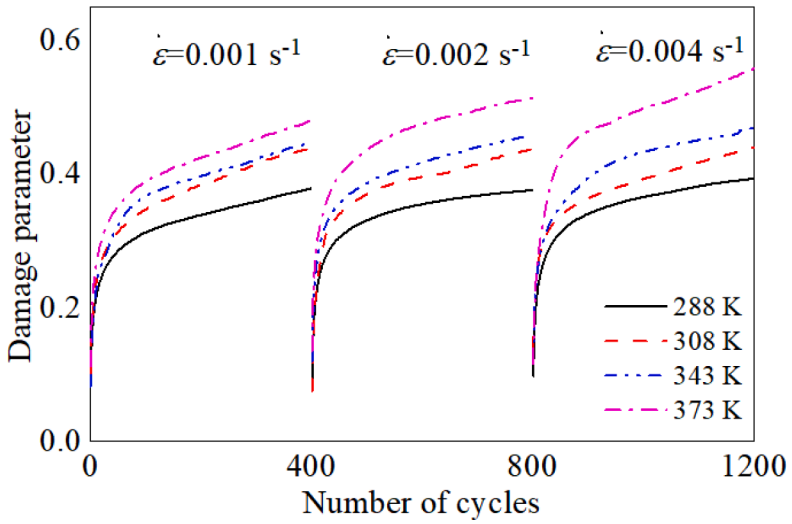

Fig. 7. Damage accumulation predicted by the proposed damage model at different temperatures of 288 K, 308 K, 343 K, and 373 K, with the applied strain rates of 0.001 s^{-1}, 0.002 s^{-1}, and 0.004 s^{-1}. The damage accumulation is promoted by the increase of strain rate and temperature.

observation of the experimented specimens. And in order to make the damage parameters more convincing, the studied damage parameters were obtained by calculating the average of the three sets of data at the most dangerous point. The trend of the damage parameter D increases as expected but in a highly nonlinear manner with the number of cycles. The loading-related parameter ζ defined in the damage parameter D in Eq. (5) could thus be calibrated to achieve a better curve fitting to the experimental results.

It should be noted that the initial value of the damage parameter was not zero because of the prescribed uniaxially tensile strain of 0.12, which was applied to SAC305 specimens ahead of strain cycles. Since SAC305 has a relatively low value of Young's modulus, the prescribed tensile strain causes irrecoverable plastic deformation in the material specimens, resulting that a certain degree of damage accumulates before the subsequent strain cycles. As a result of the thermal softening effect, the higher temperature results in more significant initial damage. It can also be concluded from Fig. 7 that the strain rate presents a promoting effect on the damage accumulation and entropy generation of SAC305 material under the same temperature conditions.

3.2. Calibration of the damage parameter

The loading-related parameter ζ in the damage parameter D is determined in Fig. 8 by cyclic loading experiments in the ranges of temperatures (288–373 K) and strain rates (0.001–0.004 s^{-1}). Therefore, a bilinear relationship between the parameter ζ, temperature and strain rate is proposed as

$$\zeta(T, \dot{\varepsilon}) = 3.005T + 9786\dot{\varepsilon} - 677.4, \tag{9}$$

where T and $\dot{\varepsilon}$ represent temperature and strain rate, respectively. Eq. (9) accommodates the determination of the damage parameters D at different temperatures and strain rates, to lay the experimental foundation for subsequent modelling for the damage-constitutive behaviour and predictions for fatigue life for Pb-free solder joints.

The evolution of damage parameter is the derivative of the damage parameter with respect to time. Unlike the damage parameter, the evolution of damage parameter indicates the instantaneous rate of damage generation accumulation, and also reveals also reveal the rate of energy dissipation during the fatigue process. Therefore, the damage

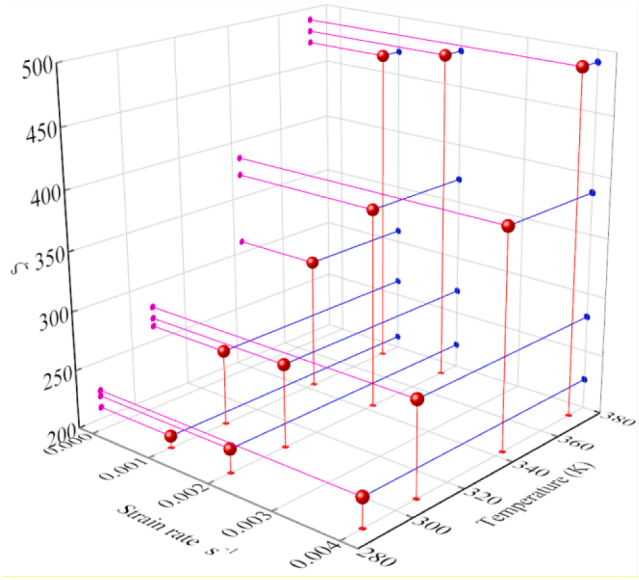

Fig. 8. Relationship between loading-related parameter ζ and strain rate for the same strain level of 0.12 at temperatures of 288 K, 308 K, 343 K, and 373 K. This insert illustrates the relationships between loading-related parameter ζ, temperature and strain rate by the way of projection.

evolution can be obtained by using EXCEL for the first order derivative with respect to time of the damage parameter that are calculated by the numerical model, and the evolution of the damage parameter are provided in Figs. 9 and 10 for SAC305 solder materials at different temperatures and the applied strain rates. The damage evolution in the first 50 cycles is emphasized, while the later cycles are excluded as the damage evolution is approximately zero and thus does not contribute much to the damage accumulation. These damage accumulation rates are significantly rapid at the beginning of the fatigue experiments. This result provides the basis for the required cyclic numbers to predict the fatigue life of SAC305 solder joints by performing finite element simulations.

In essence, the inelastic strain energy density decreases at a faster rate at lower temperatures and higher strain rates, implying faster entropy generation and faster damage accumulation. Compared with the temperature effect in Fig. 9, the effect of strain rate in Fig. 10 is more significant for describing the damage evolution in the time history. The damage accumulation of SAC305 solder at lower strain rates is slower, and thus its fatigue life is longer. In addition, the difference in the evolution of damage parameter at different temperatures is larger at low strain rates as shown in the insets of Fig. 9. With the increase in fatigue cycles, the difference in damage evolution resulting from different temperatures disappears, similar to those shown in Fig. 10. This trend is essentially the same at different temperatures and thus is considered independent of temperature conditions. This observation suggests that the evolution of the damage parameter is more associated with the applied strain rate than the temperature.

4. Microstructure observation and discussion

Based on optical microscopy, the microstructure of the fatigue-tested SAC305 solder specimens at different temperatures and strain rates are

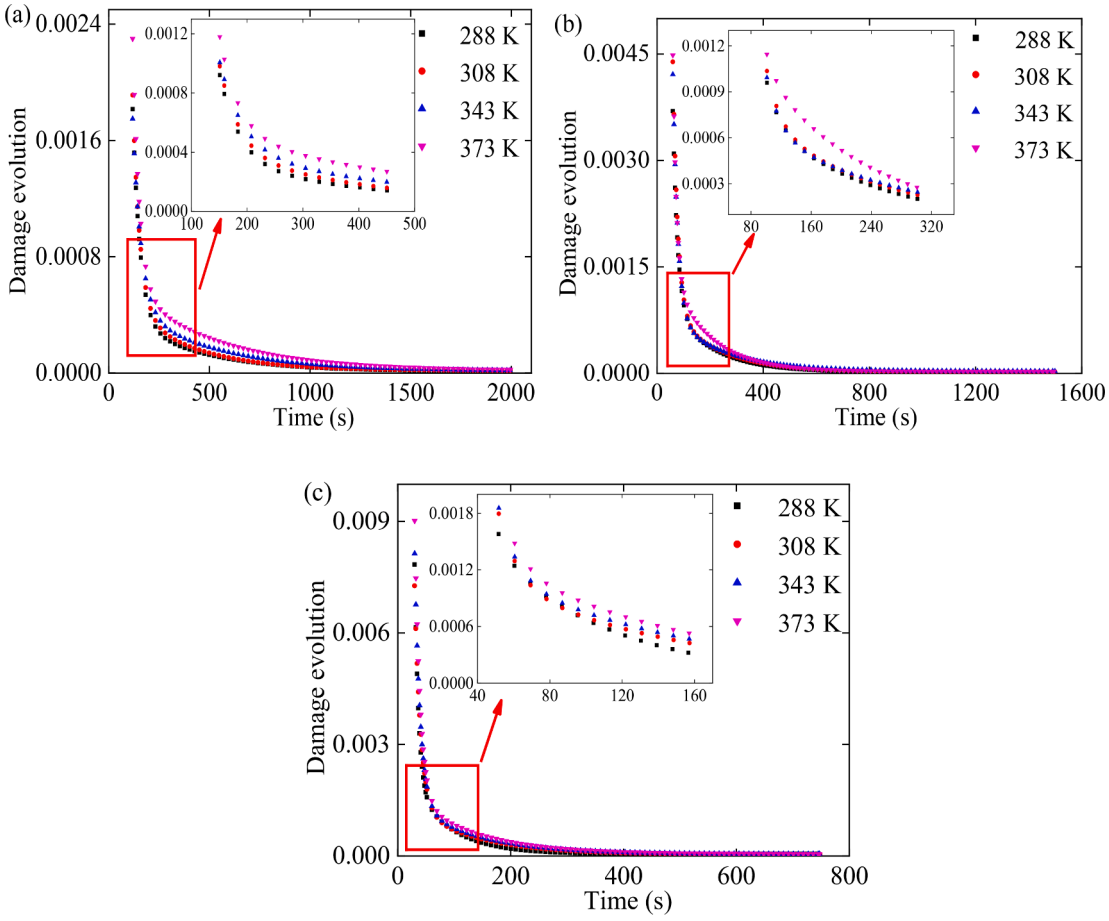

Fig. 9. Evolution of damage parameter at different temperatures of 288 K, 308 K, 343 K, and 373 K, with the applied strain rates of (a) 0.001 s^{-1}, (b) 0.002 s^{-1}, and (c) 0.004 s^{-1}. The insets show the detailed comparisons of the evolution of damage at various temperatures.

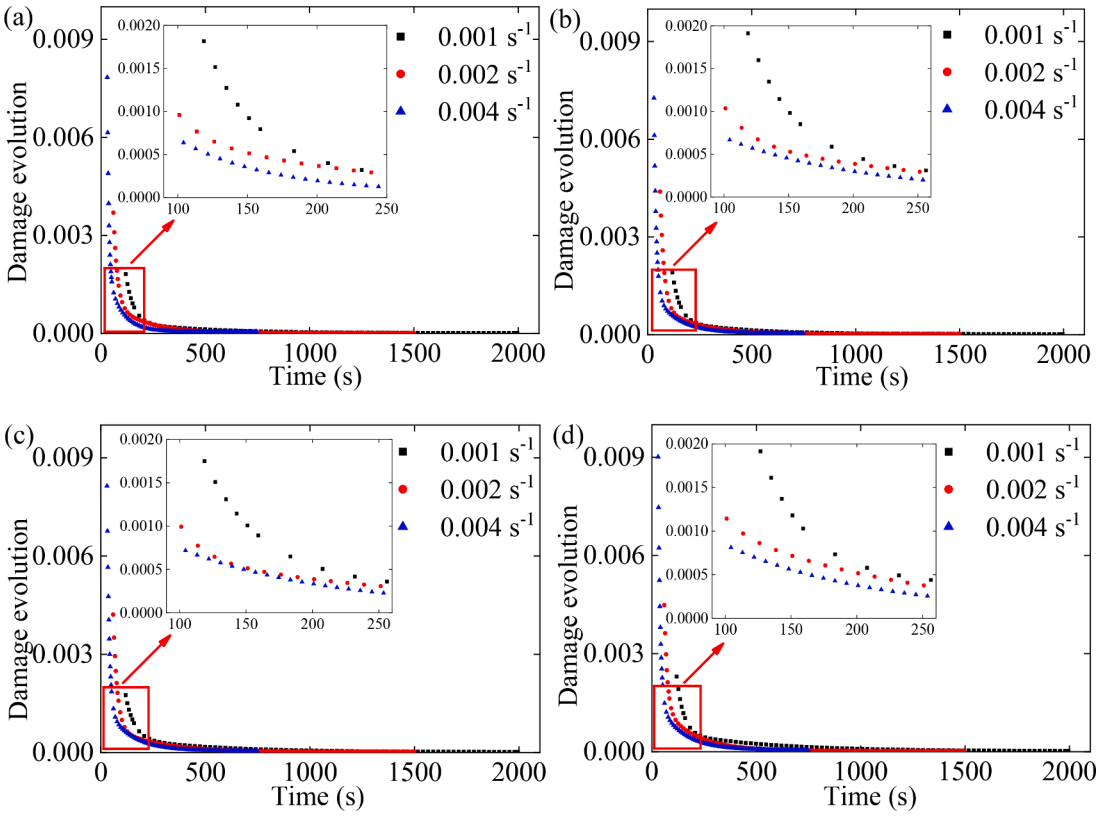

Fig. 10. Evolution of damage parameter at different strain rates of 0.001 s^{-1}, 0.002 s^{-1}, and 0.004 s^{-1}, with the applied temperatures of (a) 288 K, (b) 308 K, (c) 343 K, and (d) 373 K. The insets depict detailed comparisons of the evolution of damage at various strain rates.

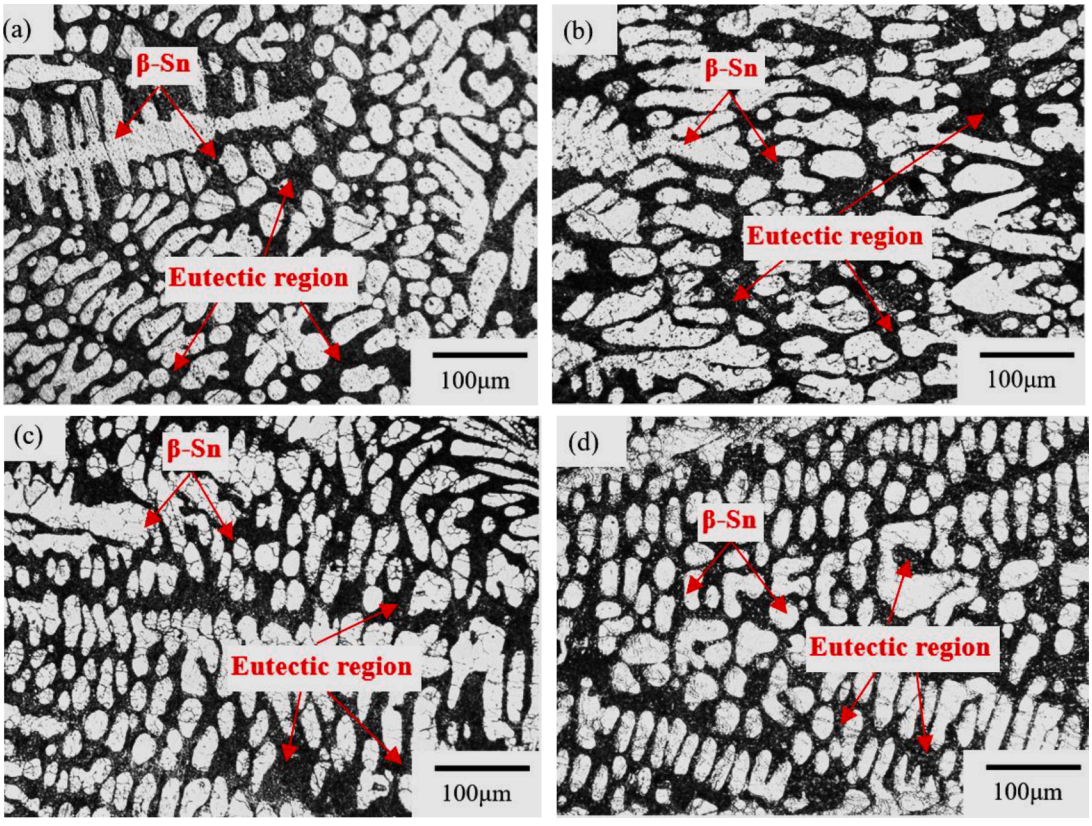

Fig. 11. Microstructural evolutions of SAC305 specimens subjected to the strain rate of 0.001s^{-1} with the applied temperatures of (a) 288 K, (b) 308 K, (c) 343 K, and (d) 373 K, demonstrating that an increase in temperature motivates β-Sn phases through thermal energy.

shown in Figs. 11 and 12, respectively. As a typical Sn-based solder material, the microstructure of as-prepared SAC305 solder comprises the dendritic β-Sn phase as the brighter zone and the surrounding Sn-Ag-Cu ternary eutectic network (*i.e.*, Cu_6Sn_5 and Ag_3Sn) as the darker zone [75–78]. The intermetallic compounds (IMCs) particles are finely distributed between these dendritic arms [75–78]. These microstructures differ for the fatigue-tested specimens at different temperatures and strain rates.

Fig. 11 shows the microstructure of SAC305 specimens with different temperatures at the strain rate of 0.001 s^{-1}. The change of β-Sn phase is focused in order to investigate the damage caused by energy dissipation of SAC305 solder at different temperatures and strain rates. It is observed that when the temperatures are 288 K and 308 K as presented in Fig. 11(a) and (b), the shape of the β-Sn phases are mostly narrow strips with large aspect ratios, and some strips are even connected to form large plates. As a result, the aspect ratios of the β-Sn phase decrease dramatically, and the shapes of most β-Sn phase almost become circular in Fig. 11(c) and (d). These comparisons suggest that as the temperature increases but with the same loading factor, the morphology of β-Sn phase dramatically change, which is apparently attributed to more active atom diffusion resulting from the increasing thermal energy [79]. When the same cyclic loading is applied to those specimens with different morphologies, the mechanical response and also the induced damage are different. Therefore, it is confirmed that more reduction in peak stress and more significant fatigue damage of SAC305 is induced at higher temperatures. Considering that the mechanical properties of SAC305 solder are also dependent on the temperature, it is challenging to explicitly explain the underlying mechanism by considering such coupled multiple factors. This outlines the significance of the present work to propose a damage model based on entropy generation. By taking advantage of the entropy generation to describe the irreversible processes (such as mass transfer processes) and thermodynamic cycle from the viewpoint of energy, the mechanical behaviour of SAC305 solder is attempted to be phenomenologically elucidated during the cyclic loading with the irreversible damage accumulation.

The specimen microstructures at the different strain rates are compared in Fig. 12. Fig. 12(a) and (b) show that when the strain rate increases from 0.001 to 0.002 s^{-1}, the microstructure become coarsened, and a few non-penetrating cracks are produced in the dendritic β-Sn phase. However, compared with the effect of temperature variations, the β-Sn phase remains mostly narrow strips with large aspect ratios as the strain rate increases. This phenomenon is supported by the observations in Fig. 12 that the damage evolution at different strain rates do not strongly depend on the temperature conditions. When the strain rate further increases, it is evident that penetrating cracks gradually appears through the dendritic β-Sn phases [80,81]. In fact, cracks appear mainly as primary cracks at low strain rates, while the secondary cracks gradually grow and the number of cracks increases as the strain rate increases in Fig. 12. In order to quantitatively describe the cracks under different strain rates, the number of cracks is counted in the representative region as shown in the yellow box of 0.01 mm^2 in Fig. 12 and is found to increase with the increase of strain rate are shown in Fig. 13. These penetrating cracks are attributed to the increase in deformation rate in the specimen due to the increasing strain rate, resulting in more dissipated energy and more significant fatigue damage in the microstructure of solder materials [79]. By correlating with the degradation trend of mechanical properties, it can be concluded that the microscopical morphologies are attributed to the entropy generation in terms of energy dissipation under the coupled effects of temperatures and strain rates.

As the present work is conducted to focus on the macroscopic damage model to accurately describe the degradation trend of mechanical properties as the outcome of multiple coupled macroscopic and mesoscopic factors, the proposed model is believed to be applicable as long as

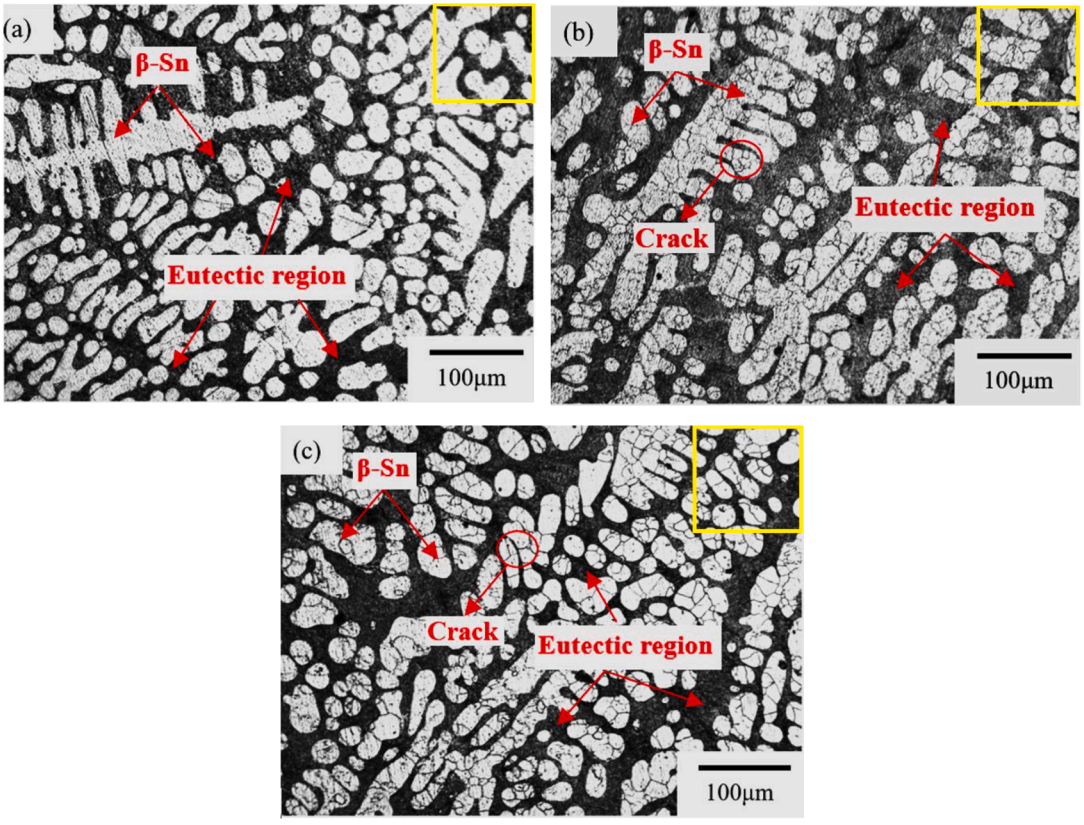

Fig. 12. Microstructural evolutions of SAC305 specimens subjected to the temperature of 288 K with the applied strain rates of (a) 0.001 s^{-1}, (b) 0.002 s^{-1}, and (c) 0.004 s^{-1}. With the increasing strain rate, the microstructural evolutions and cracks in the dendritic β-Sn phases result in entropy generation and fatigue damage.

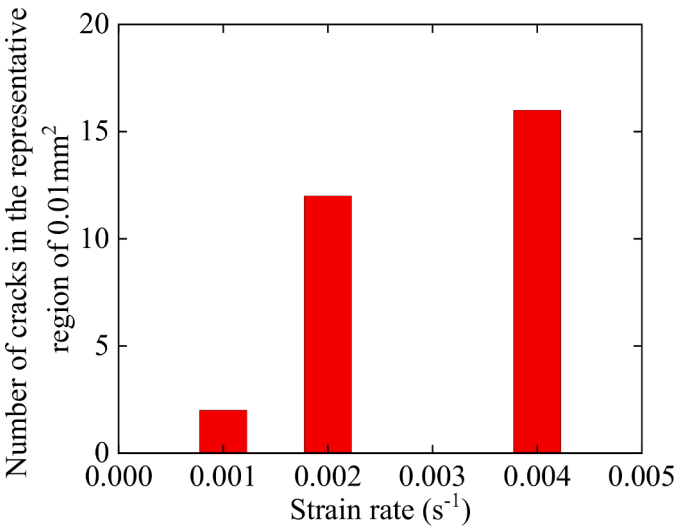

Fig. 13. Number of cracks in the representative region of 0.01mm^2 at different strain rates of 0.001 s^{-1}, 0.002 s^{-1}, and 0.004 s^{-1}. The insert provides a quantitative analysis of crack extension at various strain rates.

the crack does not propagate at the macro-scale to induce a macroscopic fracture of the SAC305 solder. Absolutely, it should be noted that some limitations and assumptions were made to simplify the proposed fatigue damage model. For instance, the tin recrystallization could be considered in the proposed entropy generation-based fatigue damage model, but the grain growth is not detailed characterized in this study. The influence of the elastic stage was neglected, so the proposed model was only applicable to low cycle fatigue with relatively large plastic strain. Future works can be performed to address the lifetime prediction for Pb-free solder under cyclic loading conditions by establishing FE simulations [82–84] based on this proposed damage model accompanied by calibrated parameters incorporated into the existing constitutive model. This enrichment could considerably improve the fatigue life estimation for electronic packaging structures and electronic devices with the thermodynamics basis of entropy generation.

For practical implementations, the proposed damage model provides a basis for coupling with the unified creep plasticity model through UMAT subroutine in the future. After comparing the prediction accuracy and computational cost of a standard dog-bone specimen in the established FE model, the optimal element size can be determined to achieve a satisfactory mesh convergence. On the basis of this, the damage accumulation during mechanical cycling of viscoplastic solder can be simulated by finite element simulation software to obtain the equivalent plastic strain increment PEEQ, and finally the fatigue life of the material can be evaluated by the Coffin-Manson model which is widely utilized in practice of electronic packaging industry.

5. Conclusions

In this study, low-cycle fatigue tests were performed on SAC305 Pb-free solders subjected to different temperatures and strain rates. According to observed degradation of peak stress, an entropy-generation damage model was proposed to relate the thermodynamic nature of the damage accumulation and evolution during a mechanical-cyclic loading. Fundamentally different from the existing empirical damage models for SAC305, the proposed approach was superior at the aspects of revealing fatigue damage in combination with microscopic evolution, which greatly enhances the physical nature when predicting fatigue life of electronic packaging structures.

As the measure of entropy generation, the peak stress degradation was reproduced by the proposed damage model and the corresponding damage evolution was computed. Greater amount and rate of mechanical degradation at the peak stress were found with the increasing temperature and strain rate. In other words, more energy was dissipated at higher temperatures and strain rates during the fatigue deformation of SAC305 solder. As the derivative of calibrated damage accumulation with changes of time, the damage evolutions were more associated with strain rates rather than the temperature. This observation had never been reported for Pb-free solder materials to the best of our knowledge. As characterized by using the optical microscopy, the shape of the β-Sn phase evolved from strips to circles with the increasing temperature. The dendritic β-Sn phase gradually coarsened with penetrating cracks with rise in temperatures and strain rates. These morphology observations confirmed that temperature and strain rate variations lead to energy dissipation, entropy generation and mechanical degradation. This trend essentially complied with the predictions by the proposed entropy-generation damage model.

CRediT authorship contribution statement

Xu Long: Methodology, Funding acquisition, Supervision, Writing – review & editing. **Ying Guo:** Investigation, Methodology, Writing – original draft, Visualization, Software. **Yutai Su:** Methodology, Software, Writing – review & editing. **Kim S. Siow:** Conceptualization, Writing – review & editing. **Chuantong Chen:** Conceptualization, Writing – review & editing.

Declaration of Competing Interest

The authors declare that they have no known competing financial interests or personal relationships that could have appeared to influence the work reported in this paper.

Acknowledgment

This work was supported by the National Natural Science Foundation of China (No. 52175148), the Natural Science Foundation of Shaanxi Province (No. 2021KW-25), and the National Key Laboratory Foundation 2022-JCJQ-LB-006 (No. 6142411232212).

References

[1] Ren J, Huang M. Board-level drop reliability and fracture behavior of low-temperature soldering Sn–Ag–Cu/Sn–Bi–X hybrid BGA solder joints for consumer electronics. J Mater Sci Mater Electron 2021;32(11):15453–65.
[2] Huang J, Zhou M, Zhang X. The melting characteristics and interfacial reactions of Sn-ball/Sn-3.0Ag-0.5Cu-paste/Cu joints during reflow soldering. J Electron Mater 2017;46(3):1504–15.
[3] Chung S, Kwak J. Comparative study on reliability and advanced numerical analysis of BGA subjected to product-level drop impact test for portable electronics. Electronics 2020;9(9):1515. Switzerland.
[4] Zeng K, Tu K. Six cases of reliability study of Pb-free solder joints in electronic packaging technology. Mater Sci Eng R 2002;38(2):55–105.
[5] Abtew M, Selvaduray G. Lead-free solders in microelectronics. Mater Sci Eng R 2000;27(5-6):95–141.
[6] Abdul-Baqi A, Schreurs P, Geers M. Fatigue damage modeling in solder interconnects using a cohesive zone approach. Int J Solids Struct 2005;42(3-4):927–42.
[7] Siswanto W, Arun M, Krasnopevtseva I, Surendar A, Maseleno A. A competition between stress triaxiality and joule heating on microstructure evolution and degradation of SnAgCu solder joints. J Manuf Process 2020;54:221–7.
[8] Tan S, Han J, Wang Y, Guo F. A method to determine the slip systems in BGA lead-free solder joints during thermal fatigue. J Mater Sci Mater Electron 2018;29(9):7501–9.
[9] Liang T, Liang Y, Fang J, Chen G, Chen X. Torsional fatigue with axial constant stress for Sn–3Ag–0.5 Cu lead-free solder. Int J Fatigue 2014;67:203–11.
[10] Kanchanomai C, Miyashita Y, Mutoh Y. Low-cycle fatigue behavior of Sn-Ag, Sn-Ag-Cu, and Sn-Ag-Cu-Bi Lead-free solders. J Electron Mater 2002;31(5):456–65.
[11] Pang J, Xiong B, Low T. Low cycle fatigue study of lead free 99.3Sn–0.7Cu solder alloy. Int J Fatigue 2004;26(8):865–72.
[12] Qiu B, et al. Survey on fatigue life prediction of BGA solder joints. Electronics 2022;11(4):542. Switz.
[13] Gharaibeh M. Optimization of dwell and ramp times for SAC305 solder thermal cycling fatigue life for testing and real-life applications. J Fail Anal Prev 2021;22(1):276–85.

[14] Moriuchi M, Kariya Y, Kondo M, Kanda Y. Class i creep deformation of Sn–Ag–Cu containing solid solution elements and its effect on thermal fatigue life of solder joints. Mater Trans 2022;63(3):805–12.
[15] Hu X, He L, Chen H, Lv Y, Gao H, Liu J. The effect of electric-thermal-vibration stress coupling on the reliability of Sn-Ag-Cu solder joints. J Electron Mater 2022; 51(1):284–94.
[16] Athamneh R, Hani D, Ali H, Hamasha S. Reliability modeling for aged SAC305 solder joints cycled in accelerated shear fatigue test. Microelectron Reliab 2020; 104:113507.
[17] Lee W, Nguyen L, Selvaduray G. Solder joint fatigue models: review and applicability to chip scale packages. Microelectron Reliab 2000;40(2):231–44.
[18] McDiarmid D. Cumulative damage in fatigue under multiaxial stress conditions. Proc Inst Mech Eng 1974;188(1):423–30.
[19] Sun B, Huang X, Xu Z. A damage evolution rate controlled method for catastrophic failure process of metal films. Mech Mater 2021;160(8):103929.
[20] Dattoma V, Giancane S, Nobile R, Panella F. Fatigue life prediction under variable loading based on a new non-linear continuum damage mechanics model. Int J Fatigue 2006;28(2):89–95.
[21] Zhou T, Chan T. Fatigue damage analysis of long span steel bridge welded members using the finite element method and damage mechanics. J Ship Mech 2009;13(5): 739–47.
[22] Zhou J, Huang H, Li Y, Guo J. A framework for fatigue reliability analysis of high-pressure turbine blades. Ann Oper Res 2019;311:489–505.
[23] Li L, Yang G, Li J. Probabilistic life calculation method of NdFeB based on brittle fatigue damage model. Comput Model Eng 2020;124(3):865–84.
[24] Asasaari S, Tamin M, Johar M, Januddi M, Kosnan M. Temperature- and strain rate-dependent damage mechanics of solder/IMC interface fracture in a ball grid array assembly. Adv Trans Eng Technol 2022;174:93–105.
[25] Gang H, An D, Jin W, Choi J. Uncertainty analysis of solder alloy material parameters estimation based on model calibration method. Microelectron Reliab 2012;52(6):1128–37.
[26] Jang J, Khonsari M. On the prediction of fatigue life subjected to variable loading sequence. Fatigue Fract Eng Mater 2021;44(11):2962–74.
[27] Zhu Z, Shen Q, Liu Y. A numerical analysis method for strength of scarf-repaired composite structure based on a bilinear damage constitutive model. Sci Technol Eng 2014;14(29):1671–815.
[28] González A, Cruchaga M, Celentano D. Bilinear damage evolution in AA2011 wire drawing processes. Int J Damage Mech 2022;31(5):645–64.
[29] Benkabouche S, Guechichi H, Amrouche A, Benkhettab B. A modified nonlinear fatigue damage accumulation model under multiaxial variable amplitude loading. Int J Mech Sci 2015;100:180–94.
[30] Larkin K, Ghommem M, Hunter A, Abdelkefi A. Nonlinear modeling and performance analysis of cracked beam microgyroscopes. Int J Mech Sci 2020;188: 105965.
[31] Shang D, Yao W. A nonlinear damage cumulative model for uniaxial fatigue. Int J Fatigue 1999;21(2):187–94.
[32] Sharma S, Sharma R, Lee J. In situ and experimental analysis of longitudinal load on carbody fatigue life using nonlinear damage accumulation. Int J Damage Mech 2022;31(4):605–22.
[33] Tang H, Basaran C. A damage mechanics-based fatigue life prediction model for solder joints. J Electron Packag 2003;125(1):120–5.
[34] Mustafa M, Roberts J, Suhling J. The effects of aging on the fatigue life of lead free solders. IEEE; 2014.
[35] Pang J, Xiong B, Low T. Low cycle fatigue models for lead-free solders. Thin Solid Films 2004;462:408–12.
[36] Kanchanomai C, Mutoh Y. Low-cycle fatigue prediction model for Pb-free solder 96.5Sn-3.5Ag. J Electron Mater 2004;33(4):329–33.
[37] Long X, Liu Y, Yao Y, Jia F, Wu Y. Constitutive behaviour and life evaluation of solder joint under the multi-field loadings. AIP Adv 2018;8(8):085001.
[38] Leslie D, Heid T, Dasgupta A. Effect of temperature on vibration fatigue of SAC105 solder material after extended room temperature aging. 2018 19th International Conference on Thermal, Mechanical and Multi-Physics Simulation and Experiments in Microelectronics and. Microsystems (EuroSimE) 2018.
[39] Cavallaro D, Greco R, Bazzano G. Effect of solder material thickness on power MOSFET reliability by electro-thermo-mechanical simulations. Microelectron Reliab 2018;88-90:1168–71.
[40] Hwang J, Kim Y, Kim J. Energy-based damage model incorporating failure cycle and load ratio effects for very low cycle fatigue crack growth simulation. Int J Mech Sci 2022;221:107223.
[41] Amiri M, Khonsari M. On the role of entropy generation in processes involving fatigue. Entropy 2012;14(1):24–31. Switz.
[42] Basaran C, Nie S. An irreversible thermodynamics theory for damage mechanics of solids. Int J Damage Mech 2004;13(3):205–23.
[43] Basaran C, Yan C. A thermodynamic framework for damage mechanics of solder joints. J Electron Mater 1998;120(4):379–84.
[44] Samal S, Moharana M. Second law analysis of recharging microchannel using entropy generation minimization method. Int J Mech Sci 2020;193:106174.
[45] Jang J, Khonsari M. On the evaluation of fracture fatigue entropy. Theor Appl Fract Mech 2018;96:351–61.
[46] Naderi M, Amiri M, Khonsari M. On the thermodynamic entropy of fatigue fracture. Proc R Soc A Math Phys 2009;466(2114):1471–2946.
[47] Liakat M, Khonsari M. Entropic characterization of metal fatigue with stress concentration. Int J Fatigue 2015;70:223–34.
[48] Krupp U, Giertler A, Koschella K. Microscopic damage evolution during very high cycle fatigue (VHCF) of tempered martensitic steel. Procedia Eng 2016;160:231–8.
[49] Hamada S, Wu H, Noguchi H. Microscopic fatigue crack behavior in precipitation strengthening stainless steel A286. Trans Jpn Soc Mech Eng A 2011;77(773): 223–7.
[50] Powers M, Pan J, Silk J, Hyland P. Effect of gold content on the microstructural evolution of SAC305 solder joints under isothermal aging. J Electron Mater 2012; 41(2):224–31.
[51] Leonid A, Sergei S. A model of mechanothermodynamic entropy in Tribology. Entropy 2017;19(3):115. Switz.
[52] Leonid A, Sergei S. Mechanothermodynamic entropy and analysis of damage state of complex systems. Entropy 2016;18(7):268. Switz.
[53] Sosnovskiy L, Sherbakov S. Mechanothermodynamical system and its behavior. Contin Mech Therm 2012;24(3):239–56.
[54] Mohammadi B, Shokrieh M, Jamali M, Mahmoudi A, Fazlali B. Damage-entropy model for fatigue life evaluation of off-axis unidirectional composites. Compos Struct 2021;270(13):114100.
[55] Ghane E, Mohammadi B. Entropy-damage mechanics for the failure investigation of plain weave fabric composites. Compos Struct 2020;250(15):112493.
[56] Mahmoudi A, Mohammadi B. Theoretical-experimental investigation of temperature evolution in laminated composites due to fatigue loading. Compos Struct 2019;225:110972.
[57] Wang J, Yao Y. An entropy-based failure prediction model for the creep and fatigue of metallic materials. Entropy 2019;21(11):1104. Switz.
[58] Long X, He X, Yao Y. An improved unified creep-plasticity model for SnAgCu solder under a wide range of strain rates. J Mater Sci 2017;52(10):6120–37.
[59] Wang W, Long X, Du C, Fu Y, Wu Y. Enhancement of the unified constitutive model for viscoplastic solders in wide strain rate and temperature ranges. Strength Mater 2020;51(8).
[60] Xu L, Chen B, Yao Y. Thermo-visco-plastic constitutive model for lead-containing and lead-free solders subjected to monotonic and cyclic loadings. In: Proceedings of the 17th international conference on electronic packaging technology (ICEPT); 2016.
[61] Xu L, Wang S, Feng Y, Yao Y, Keer L. Annealing effect on residual stress of Sn-3.0Ag-0.5Cu solder measured by nanoindentation and constitutive experiments. Mater Sci Eng A 2017;696:90–5.
[62] Long X, Tang W, Wang S, Yao Y. Annealing effect to constitutive behavior of Sn-3.0Ag-0.5Cu solder. J Mater Sci Mater Electron 2018;29(9):7177–87.
[63] Ma H. Constitutive models of creep for lead-free solders. J Mater Sci 2009;44(14): 3841–51.
[64] Qin F, An T, Chen N. Strain rate effects and rate-dependent constitutive models of lead-based and lead-free solders. J Appl Mech 2010;77(1):011008-1-011008-11.
[65] Xie M, Chen G, Yang J, Xu W. Temperature- and rate-dependent deformation behaviors of SAC305 solder using crystal plasticity model. Mech Mater 2021;157: 103834.1-103834.10.
[66] Sadiq M, Pesci R, Cherkaoui M. Impact of thermal aging on the microstructure evolution and mechanical properties of lanthanum-doped tin-silver-copper lead-free solders. J Electron Mater 2013;42(3):492–501.
[67] Temfack T, Basaran C. Experimental verification of thermodynamic fatigue life prediction model using entropy as damage metric. Mater Sci Technol Lond 2015;31 (13b):1627–32.
[68] Boltzmann L, Brush S, Balazs N. Lectures on gas theory. Am J Phys 1964;17(9):68.
[69] Basaran C, Hong T. Implementation of a thermodynamic framework for damage mechanics of solder interconnects in microelectronic packaging. Int J Damage Mech 2002;11(1):87–108.
[70] Basaran C, Lin M, Hua Y. A thermodynamic model for electrical current induced damage. Int J Solids Struct 2003;40(26):7315–27.
[71] Krajcinovic D. Continuum damage mechanics. Appl Mech Rev 1984;37(1):1–6.
[72] Long X, et al. Effect of Temperature on the Fatigue Damage of SAC305 Solder. In: Proceedings of the 22nd international conference on electronic packaging technology (ICEPT). IEEE; 2021.
[73] Shi X, Pang H, Zhou W, Wang Z. Low cycle fatigue analysis of temperature and frequency effects in eutectic solder alloy. Int J Fatigue 2000;22(3):217–28.
[74] Kanchanomai C, Mutoh Y. Effect of temperature on isothermal low cycle fatigue properties of Sn–Ag eutectic solder. Mater Sci Eng A 2004;381(1-2):113–20.
[75] Yasmeen T, Sadiq M, Khan M. Effect of lanthanum doping on the microstructure evolution and intermetallic compound (IMC) growth during Thermal aging of SAC305 solder alloy. Mater Sci Eng 2014;3(2).
[76] Lu T, Yi D, Wang H, Tu X, Wang B. Microstructure, mechanical properties, and interfacial reaction with Cu substrate of Zr-modified SAC305 solder alloy. J Alloy Compd 2019;781:633–43.
[77] Cheng F, Nishikawa H, Takemoto T. Microstructural and mechanical properties of Sn–Ag–Cu lead-free solders with minor addition of Ni and/or Co. J Mater Sci 2008; 43(10):3643–8.
[78] Xu Y, et al. A multi-scale approach to microstructure-sensitive thermal fatigue in solder joints. Int J Plast 2022;155:103308.
[79] Chen B, Jiang J, Dunne F. Is stored energy density the primary meso-scale mechanistic driver for fatigue crack nucleation? Int J Plast 2017;101:213–29.
[80] Zhai T, Jiang X, Li J, Garratt M, Bray G. The grain boundary geometry for optimum resistance to growth of short fatigue cracks in high strength Al-alloys. Int J Fatigue 2005;27(10-12):1202–9.
[81] Han Q, et al. Crystal orientation effect on fretting fatigue induced geometrically necessary dislocation distribution in Ni-based single-crystal superalloys. Acta Mater 2019;179(15):129–41.

[82] Wang W, Yao Y, Long X, Zhu Z. Material and structural optimization of fatigue life of PBGA under temperature cycling. 19th International Conference on Electronic Packaging Technology (ICEPT). 2018.
[83] Wang W, Chen Z, Wang S, Long X. Mechanics-based acceleration for estimating thermal fatigue life of electronic packaging structure. Microelectron Reliab 2020; 107:113616.
[84] Yang B, Luo J, Wan B, Su Y, Fu G, Long X. Numerical and Experimental Investigations of the Thermal Fatigue Lifetime of CBGA Packages. Comp Model Eng Sci 2022;130(2):1113–34.